

Synthesis, Structures, and Antibacterial Activities of Two Iron(III) Complexes with Schiff Bases¹

F. Y. Wei* and P. H. Wen

Department of Chemistry and Chemical Engineering, Baoji University of Arts and Sciences, Baoji, 721013 P.R. China

*e-mail: weifenyang78@163.com

Received July 25, 2013

Abstract—Two Schiff base iron(III) complexes, $[\text{FeL}^1(\text{AHA})] \cdot \text{H}_2\text{O}$ (**I**) and $[\text{Fe}(\text{L}^2)_2] \cdot \text{ClO}_4$ (**II**), where AHA is the deprotonated form of acetohydroxamic acid, and L^1 and L^2 are the anionic form of *N,N'*-bis(3-ethoxysalicylidene)propane-1,2-diamine and 2-[1-(2-aminopropylimino)ethyl]phenol, respectively, have been synthesized and characterized by physical chemical methods and single crystal X-ray diffraction. Crystallographic data for **I**: orthorhombic, space group *Iba*2, $a = 20.781(3)$, $b = 23.527(3)$, $c = 10.071(2)$ Å, $V = 4923.7(12)$ Å³, $Z = 8$, $R_1 = 0.0374$, $wR_2 = 0.0900$. Crystallographic data for **II**: triclinic, space group *P*1̄, $a = 12.748(1)$, $b = 13.401(1)$, $c = 19.007(1)$ Å, $\alpha = 106.623(2)^\circ$, $\beta = 97.462(2)^\circ$, $\gamma = 112.543(2)^\circ$, $V = 2784.9(4)$ Å³, $Z = 4$, $R_1 = 0.0892$, $wR_2 = 0.2434$. X-ray crystal structural study indicated that the coordination environment around each Fe atom in the complexes is a six-coordinated distorted octahedron. The antibacterial activities of the complexes were assayed.

DOI: 10.1134/S1070328414040113

INTRODUCTION

Iron is an important element for biological processes of human beings [1–3]. Iron is also an essential cofactor in metalloenzymes [4]. Its importance in DNA synthesis, control of gene expression, and induction of cell apoptosis is becoming better understood [5]. Schiff bases derived from benzaldehydes with various organic amines are important ligands in the coordination of transition metal atoms. Iron complexes with Schiff bases have been received particular interest for their biological effects, especially antibacterial and antitumor activities [6–10]. However, when compared to other transition metal ions, the number of complexes bearing iron centers is much less. In the present work, two new iron(III) complexes, $[\text{FeL}^1(\text{AHA})] \cdot \text{H}_2\text{O}$ (**I**) and $[\text{Fe}(\text{L}^2)_2] \cdot \text{ClO}_4$ (**II**), where AHA is the deprotonated form of acetohydroxamic acid, and L^1 and L^2 are the anionic form of *N,N'*-bis(3-ethoxysalicylidene)propane-1,2-diamine (H_2L^1) and 2-[1-(2-aminopropylimino)ethyl]phenol (HL^2), respectively, have been synthesized, characterized, and investigated for their antibacterial activities.

EXPERIMENTAL

All chemical reagents and solvents were of analytical grade and were obtained from Sigma-Aldrich. Methanol was dried over molecular sieves (4 N) prior to use. Elemental analyses were performed on a PerkinElmer 2400 II elemental analyzer. Infrared

spectra were recorded on a PerkinElmer RX I FT-IR spectrophotometer with KBr discs. TG–DTA analysis was carried out under nitrogen with a heating rate of $10^\circ\text{C min}^{-1}$ using a Perkin Elmer Pyris Diamond TG/DTA analyzer.

Iron perchlorate is potentially explosive, only small quantity should be used and handled with great care.

Synthesis of the Schiff bases. The Schiff bases H_2L^1 and HL^2 were synthesized by refluxing hot ethanolic solution (30 mL) of propane-1,2-diamine (0.01 mol) with 3-ethoxysalicylaldehyde (0.02 mol) and 2-acetylphenol (0.02 mol), respectively for about 1 h. The precipitates formed during reflux were filtered, washed with cold EtOH, and recrystallized from hot EtOH. The yields were 83 and 77% for H_2L^1 and HL^2 , respectively.

For $\text{C}_{21}\text{H}_{26}\text{N}_2\text{O}_4$ (H_2L^1)

anal. calcd., %:	C, 68.1;	H, 7.1;	N, 7.6.
Found, %:	C, 67.9;	H, 7.2;	N, 7.5.

For $\text{C}_{11}\text{H}_{16}\text{N}_2\text{O}$ (HL^2)

anal. calcd., %:	C, 68.7;	H, 8.4;	N, 14.6.
Found, %:	C, 68.6;	H, 8.3;	N, 14.4.

Synthesis of complex I. A methanolic solution (10 mL) of H_2L^1 (0.1 mmol, 37.0 mg) was mixed with a methanolic solution (10 mL) of $\text{Fe}(\text{ClO}_4)_3$ (0.1 mmol, 37.2 mg) and acetohydroxamic acid (0.1 mmol, 7.5 mg), and refluxed in a water bath for

¹ The article is published in the original.

1 h. Single crystals suitable for X-ray diffraction were obtained by slow evaporation of the solution in air for a few days. The yield was 43%.

For $C_{23}H_{30}N_3O_7Fe$

anal. calcd., %: C, 53.5; H, 5.9; N, 8.1.
Found, %: C, 53.7; H, 6.0; N, 8.1.

Synthesis of complex II. A methanolic solution (10 mL) of HL^2 (0.1 mmol, 19.2 mg) was mixed with a methanolic solution (10 mL) of $Fe(ClO_4)_3$ (0.1 mmol, 37.2 mg), and refluxed in a water bath for 1 h. Single crystals suitable for X-ray diffraction were obtained by slow evaporation of the solution in air for a few days. The yield was 65%.

For $C_{22}H_{30}N_4O_6ClFe$

anal. calcd., %: C, 49.1; H, 5.6; N, 10.4.
Found, %: C, 49.0; H, 5.7; N, 10.2.

Single crystal X-ray diffraction. X-ray data for the complexes were collected on a Bruker SMART APEXII diffractometer equipped with graphite-monochromated MoK_α radiation ($\lambda = 0.71073 \text{ \AA}$). A preliminary orientation matrix and cell parameters were determined from three sets of ω scans at different starting angles. Data frames were obtained at scan intervals of 0.5° with an exposure time of 10 s frame^{-1} . The reflection data were corrected for Lorentz and polarization factors. Absorption corrections were carried out using SADABS. The structures were solved by direct methods and refined by full-matrix least-squares analysis using anisotropic thermal parameters for non-H atoms with the SHELXTL program [11]. All H atoms were calculated at idealized positions and refined with the riding models. Crystallographic data for the complexes are summarized in Table 1.

Supplementary material has been deposited with the Cambridge Crystallographic Data Centre (nos. 950909 (I) and 950910 (II); deposit@ccdc.cam.ac.uk or <http://www.ccdc.cam.ac.uk>).

Antibacterial activity test. The in vitro activity test was carried out using the growth inhibitory zone (well method) [12]. The potency of components was determined against the Gram-positive bacteria: *S. agalactiae* and *S. aureus* and the Gram-negative bacteria: *K. pneumoniae* and *P. aeruginosa*. Microorganisms were cultured on Muller–Hinton agar medium. The inhibitory activity was compared with that of standard antibiotics, such as gentamicine (10 μg). After drilling wells on medium using a 6 mm cork borer, 100 μL of solution from different compounds were poured into each well. The plates were incubated at 37°C overnight. The diameter of the inhibition zone was measured to the nearest. Each test was carried out in triplicate and the average was calculated for inhibition zone diameters. A blank containing only methanol

showed no inhibition in a preliminary test. The macro-dilution broth susceptibility assay was used for the evaluation of minimal inhibitory concentration (MIC). By including 1 mL Muller–Hinton broth in each test, and then adding 1 mL extract with concentration 100 mg/mL in the first tube, we made serial dilution of this extract from first tube to last tube. Bacterial suspension prepared to match the turbidity of 0.5 Mcfarland turbidity standards. Matching this turbidity provides a bacterial inoculum concentration of $1.5 \times 10^8 \text{ cfu/mL}$. Then 1 mL of bacterial suspension was added to each test tube. After incubation at 37°C for 24 h, the last tube was determined as the minimal inhibitory concentration (MIC) without turbidity.

RESULTS AND DISCUSSION

Two new mononuclear iron(III) complexes were synthesized by reaction of Schiff bases, acetohydroxamic acid, with iron perchlorate in methanol. For complex I, acetohydroxamic acid was coordinated to the Fe atom, while for complex II, even though we had added the material, it has not participated in coordination.

The asymmetric unit of compound I contains a mononuclear iron complex molecule and a water molecule of crystallization (Fig. 1a). The Fe atom in the complex shows distorted octahedral coordination geometry, with O(1), N(2) atoms of the Schiff base ligand, and O(5) and O(6) atoms of the AHA ligand defining the equatorial coordination sites, and N(1) and O(2) atoms of the Schiff base ligand occupying the axial positions. The Fe atom deviates from the best coordination plane defined by the equatorial atoms by $0.145(1) \text{ \AA}$ in direction of O(2) atom. The coordinate bond lengths and angles (Table 2) are in line with the corresponding values found in related six-coordinated iron(III) complexes with Schiff bases [13, 14]. The distortion of the octahedral coordination may be caused by the strain created by the five-membered chelate rings $Fe(1)-N(1)-C(8)-C(9)-N(2)$ and $Fe(1)-O(5)-C(22)-N(3)-O(6)$. The three *trans* angles are much deviated from the ideal value of 180° , ranging from $155.9(1)^\circ$ to $161.7(1)^\circ$. The remaining bond angles are also deviated from the ideal value of 90° , ranging from $74.4(1)^\circ$ to $112.4(1)^\circ$. The dihedral angle between the two benzene rings of the Schiff base ligand is $33.5(3)^\circ$.

In the crystal structure of complex I, the iron complex molecules and the water molecules are linked together by $O-H\cdots O$ and $N-H\cdots O$ hydrogen bonds (Table 3), to form 2D layers parallel to the yz plane (Fig. 2a).

The asymmetric unit of compound II contains two mononuclear iron complex cations and two perchlorate anions (Fig. 1b). The Fe atom in the complex shows distorted octahedral coordination geometry, with the three donor atoms of one Schiff base ligand and the imino N atom of the other Schiff base ligand

Table 1. Crystallographic data and experimental details for structures **I** and **II**

Parameter	Value	
	I	II
Formula weight	516.35	537.80
Crystal size, mm	0.30 × 0.27 × 0.27	0.30 × 0.27 × 0.27
Temperature, K	298(2)	298(2)
Crystal system	Orthorhombic	Triclinic
Space group	<i>Iba2</i>	<i>P</i> $\bar{1}$
<i>a</i> , Å	20.781(3)	12.748(1)
<i>b</i> , Å	23.527(3)	13.491(1)
<i>c</i> , Å	10.071(2)	19.007(1)
α , deg	90	106.623(2)
β , deg	90	97.462(2)
γ , deg	90	112.543(2)
<i>V</i> , Å ³	4923.7(12)	2784.9(4)
<i>Z</i>	8	4
ρ_{calcd} , mg cm ⁻³	1.393	1.283
$\mu(\text{MoK}\alpha)$, mm ⁻¹	0.660	0.677
<i>F</i> (000)	2168	1124
Number of measured reflections	24588	26141
Number of observations (<i>I</i> > 2 σ (<i>I</i>))	5071	10319
Unique reflections	4132	5591
Parameters	320	616
Number of restraints	5	48
<i>R</i> ₁ , <i>wR</i> ₂ (<i>I</i> > 2 σ (<i>I</i>))*	0.0374, 0.0900	0.0892, 0.2434
<i>R</i> ₁ , <i>wR</i> ₂ (all data)*	0.0534, 0.0999	0.1632, 0.2942
Goodness of fit of <i>F</i> ²	1.043	1.020
Largest difference peak and hole, <i>e</i> Å ⁻³	0.280, -0.271	0.799, -0.572

* $R_1 = \sum |F_o| - |F_c| / \sum |F_o|$, $wR_2 = [\sum w(F_o^2 - 2F_c^2)^2 / \sum w(F_o^2)^2]^{1/2}$.

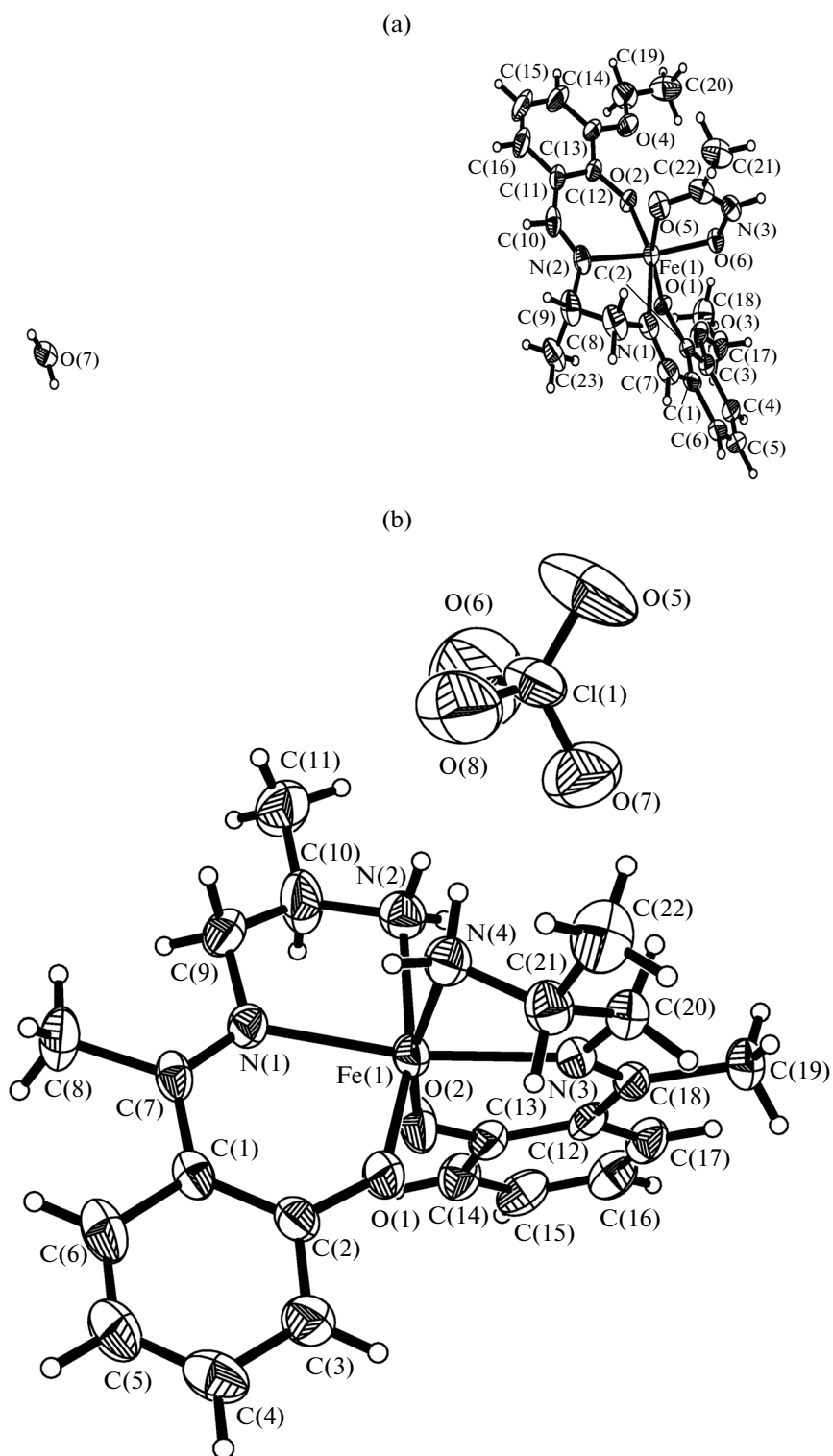


Fig. 1. ORTEP diagram of complexes I (a) and II (b) with 30% thermal ellipsoids for all non-hydrogen atoms.

defining the equatorial coordination sites, and the remaining two donor atoms of the second Schiff base ligand occupying the axial positions. The Fe(1) and Fe(2) atoms deviate from the best coordination planes

defined by the equatorial atoms by 0.095(1) Å and 0.116(1) Å, respectively. The coordinate bond lengths and angles (Table 2) are comparable to those observed in complex I, and also in line with the corresponding

values found in related six-coordinated iron(III) complexes with Schiff bases [15, 16]. The distortion of the octahedral coordination may be caused by the strain created by the five-membered chelate rings Fe(1)–N(1)–C(9)–C(10)–N(2), Fe(1)–N(3)–C(20)–C(21)–N(4), Fe(2)–N(5)–C(31)–C(2)–N(6), and Fe(2)–N(7)–C(42)–C(43)–N(8). The three *trans* angles are much deviated from the ideal value of 180°, ranging from 164.7(2)° to 170.4(2)° for Fe(1) and from 162.7(2)° to 168.9(2)° for Fe(2). The remaining bond angles are also deviated from the ideal value of 90°, ranging from 78.5(2)° to 100.1(2)° for Fe(1) and from 77.8(2)° to 100.8(2)° for Fe(2). The two Schiff base ligands in the complex are also vertical to each other, with dihedral angles of 99.6(3)° for Fe(1) complex molecule, and 108.0(3)° for Fe(2) complex molecule.

In the crystal structure of complex **II**, the complex cations and the perchlorate anions are linked together by N–H···O hydrogen bonds (Table 3), to form dimers (Fig. 2b).

The infrared spectra of the Schiff bases and their complexes provide information about the metal–ligand bonding. The medium and broad absorptions in the 3200–3500 cm⁻¹ region for the Schiff bases and complex **I** substantiate the presence of O–H groups. The sharp and weak absorptions at 3227 and 3258 cm⁻¹ for complexes **I** and **II** are assigned to N–H groups. Strong absorptions at 1645 cm⁻¹ for H₂L¹ and 1639 cm⁻¹ for HL² are assigned to the azomethine groups, $\nu(\text{C}=\text{N})$ [17]. The bands appeared at 1633 cm⁻¹ for **I** and 1636 cm⁻¹ for **II**, which can be attributed to donation of the nitrogen atom lone pair of the azomethine groups to the metal ions. The phenolic $\nu(\text{C}-\text{O})$ in the free Schiff base ligands exhibit strong bands at 1262 cm⁻¹ for H₂L¹ and 1253 cm⁻¹ for HL². In the complexes, the bands appear at lower wave numbers, viz. 1243 cm⁻¹ for **I** and 1235 cm⁻¹ for **II**, when compared to those of the free Schiff bases. In the spectrum of **II**, the intense band centered at 1115 cm⁻¹ is attributed to the perchlorate anions. Conclusive evidence of the bonding is also shown by the presence of new bands in the spectra of the complexes at about 520–570 and 410–490 cm⁻¹, which can be attributed to $\nu(\text{Fe}-\text{O})$ and $\nu(\text{Fe}-\text{N})$ stretching vibrations, respectively [18].

TG–DTA curves of complex **I** are shown in Fig. 3a. The mass loss corresponding to one lattice water molecule is observed at 100–170°C. The organic part of the complex decomposes into roughly two steps, the first lies in the range 170–218°C with a DTG peak at 222°C. The mass loss (14.0%) corresponds to loss of the AHA ligand. The next stage of decomposition starts at 220°C and ends at 450°C. Since the TG curve of the complex showed continuous degradation at this stage, we were not able to isolate the intermediates. The steady mass loss observed at this stage may be due

Table 2. Selected bond lengths (Å) and angles (deg) for **I** and **II**

Bond	<i>d</i> , Å	Bond	<i>d</i> , Å
I			
Fe(1)–O(1)	1.969(2)	Fe(1)–O(2)	1.933(2)
Fe(1)–O(5)	2.084(2)	Fe(1)–O(6)	1.9657(18)
Fe(1)–N(1)	2.113(3)	Fe(1)–N(2)	2.189(3)
II			
Fe(1)–O(1)	1.881(5)	Fe(1)–O(2)	1.888(5)
Fe(1)–N(1)	2.143(5)	Fe(1)–N(2)	2.176(6)
Fe(1)–N(3)	2.133(5)	Fe(1)–N(4)	2.148(6)
Fe(2)–O(3)	1.899(5)	Fe(2)–O(4)	1.882(5)
Fe(2)–N(5)	2.136(5)	Fe(2)–N(6)	2.161(6)
Fe(2)–N(7)	2.144(5)	Fe(2)–N(8)	2.163(5)
Angle	ω , deg	Angle	ω , deg
I			
O(2)Fe(1)O(6)	103.3(1)	O(2)Fe(1)O(1)	94.0(1)
O(6)Fe(1)O(1)	86.0(1)	O(2)Fe(1)O(5)	98.4(1)
O(6)Fe(1)O(5)	78.2(1)	O(1)Fe(1)O(5)	161.7(1)
O(2)Fe(1)N(1)	155.9(1)	O(6)Fe(1)N(1)	100.6(1)
O(1)Fe(1)N(1)	84.6(1)	O(5)Fe(1)N(1)	89.4(1)
O(2)Fe(1)N(2)	84.1(1)	O(6)Fe(1)N(2)	159.9(1)
O(1)Fe(1)N(2)	112.4(1)	O(5)Fe(1)N(2)	82.3(1)
N(1)Fe(1)N(2)	74.4(1)		
II			
O(1)Fe(1)O(2)	96.2(3)	O(1)Fe(1)N(3)	100.1(2)
O(2)Fe(1)N(3)	86.7(2)	O(1)Fe(1)N(1)	86.3(2)
O(2)Fe(1)N(1)	99.8(2)	N(3)Fe(1)N(1)	170.4(2)
O(1)Fe(1)N(4)	90.4(2)	O(2)Fe(1)N(4)	164.7(2)
N(3)Fe(1)N(4)	78.5(2)	N(1)Fe(1)N(4)	94.3(2)
O(1)Fe(1)N(2)	165.6(2)	O(2)Fe(1)N(2)	88.8(2)
N(3)Fe(1)N(2)	93.7(2)	N(1)Fe(1)N(2)	79.5(2)
N(4)Fe(1)N(2)	88.2(2)	O(4)Fe(2)O(3)	96.7(3)
O(4)Fe(2)N(5)	100.8(2)	O(3)Fe(2)N(5)	85.2(2)
O(4)Fe(2)N(7)	86.2(2)	O(3)Fe(2)N(7)	102.7(2)
N(5)Fe(2)N(7)	168.9(2)	O(4)Fe(2)N(6)	89.3(3)
O(3)Fe(2)N(6)	162.7(2)	N(5)Fe(2)N(6)	77.8(2)
N(7)Fe(2)N(6)	93.8(2)	O(4)Fe(2)N(8)	164.6(2)
O(3)Fe(2)N(8)	89.8(2)	N(5)Fe(2)N(8)	93.5(2)
N(7)Fe(2)N(8)	78.8(2)	N(6)Fe(2)N(8)	88.4(2)

Table 3. Geometric parameters of hydrogen bonds for **I** and **II***

D–H...A	Distance, Å			Angle DHA, deg
	D–H	H...A	D...A	
I				
O(7)–H(7B)...O(3) ⁱ	0.85(1)	2.31(2)	3.026(4)	144(3)
O(7)–H(7B)...O(1) ⁱ	0.85(1)	2.31(2)	3.044(3)	147(3)
N(3)–H(3)...O(7) ⁱⁱ	0.90(1)	1.92(1)	2.810(4)	171(4)
II				
N(8)–H(8B)...O(6)	0.90	2.41	3.28(2)	160
N(8)–H(8A)...O(11) ⁱⁱⁱ	0.90	2.16	3.04(1)	167
N(6)–H(6B)...O(9) ^{iv}	0.90	2.37	3.15(1)	146
N(6)–H(6A)...O(9) ⁱⁱⁱ	0.90	2.35	3.21(2)	158
N(4)–H(4B)...O(8) ⁱⁱⁱ	0.90	2.31	3.06(1)	140
N(4)–H(4A)...O(8)	0.90	2.34	3.23(1)	168
N(2)–H(2A)...O(6)	0.90	2.52	3.27(2)	142
N(2)–H(2A)...O(7)	0.90	2.44	3.16(1)	138

* Symmetry codes: ⁱ $x, 1 - y, -1/2 + z$; ⁱⁱ $x, -1 + y, z$; ⁱⁱⁱ $1 - x, 2 - y, 1 - z$; ^{iv} $x, y, -1 + z$.

to the removal of the Schiff base ligand, and the formation of final product (Fe₂O₃).

TG–DTA curves of complex **II** are shown in Fig. 3b. The mass loss corresponding to one perchlorate anion is observed at 110–160°C. The organic part of the complex decomposes into roughly two steps, the first lies in the range 208–240°C with a DTG peak at 218°C. The mass loss (50.0%) corresponds to loss of the four outer atoms of the benzene rings and the methyl atoms of the Schiff base ligands. The next stage of decomposition starts at 240°C and ends at 460°C. The steady mass loss observed at this stage may be due to the removal of the remaining parts of the Schiff base ligands, and the formation of final product (Fe₂O₃).

Antibacterial activities of the Schiff bases and the two complexes as well as the reference drug gentamicine are summarized in Table 4 (zone of growth inhibition and minimal inhibitory concentrations). The results indicate strong activity of the free Schiff bases against Gram-positive bacteria, *S. agalactiae*, and moderate activities of them toward Gram-positive bacteria *S. aureus* and Gram-negative bacteria *K. pneumoniae* and *P. aeruginosa*. In comparison, the iron complexes have stronger activities against all the bacteria than the free Schiff bases. The increased activity of the complexes may be explained on the basis of chelation theory; chelation reduces the polarity of the metal atom mainly because of partial sharing of its positive charge with the donor groups and possible

Table 4. Growth inhibition zone (mm) and MIC (mg/mL) values (in brackets) of compounds H₂L¹, HL², **I**, and **II**

Gram-positive and -negative bacteria	Gentamicine	H ₂ L ¹	HL ²	I	II
<i>S. agalactiae</i>		20 (25)	10 (50)	30 (6.25)	30 (12.5)
<i>S. aureus</i>	20	10 (25)	10 (25)	40 (3.125)	30 (6.25)
<i>K. pneumoniae</i>	20	20 (12.5)	20 (12.5)	30 (6.25)	40 (3.125)
<i>P. aeruginosa</i>	15	10 (50)	10 (25)	30 (12.5)	20 (12.5)

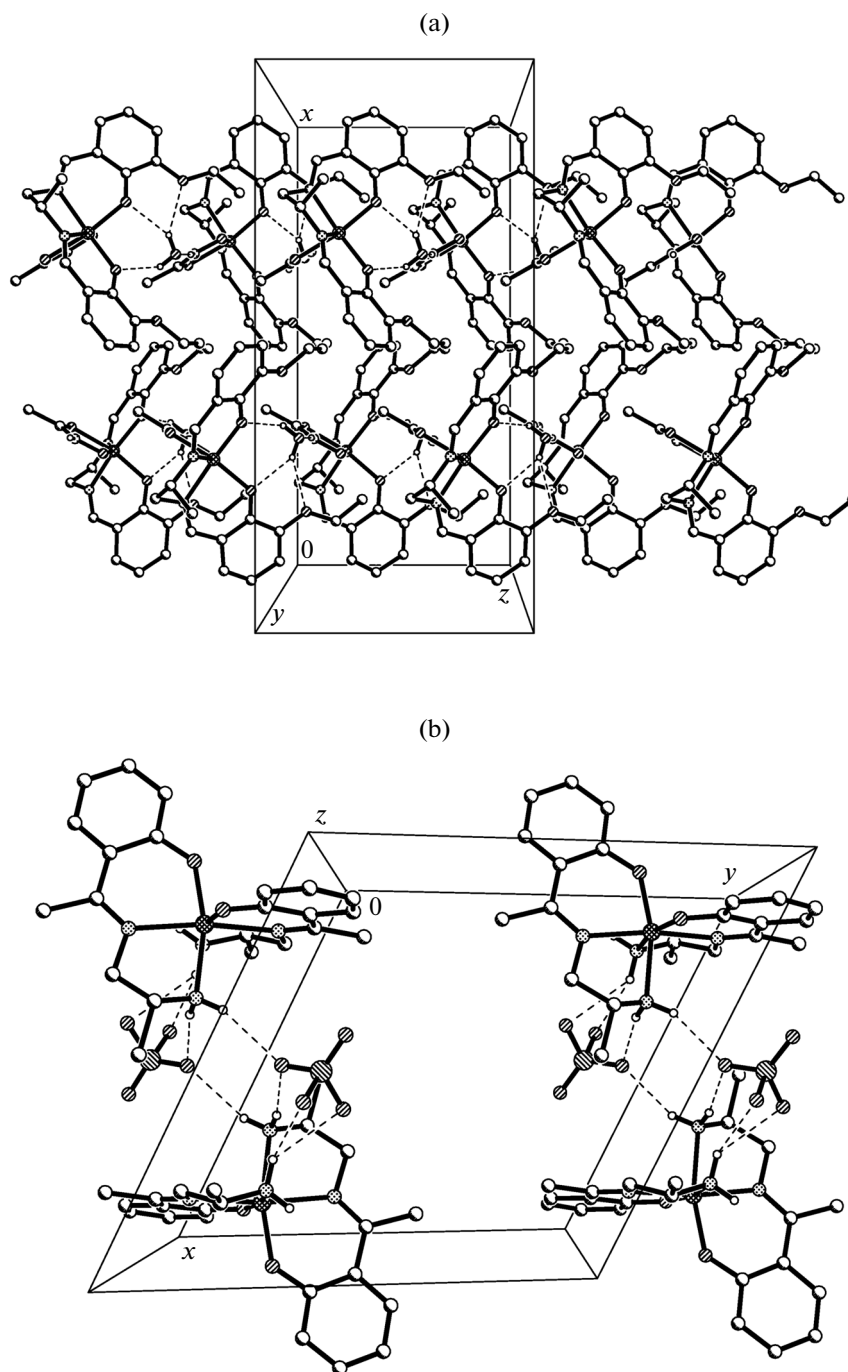


Fig. 2. Molecular packing structure of complexes I (a) and II (b), viewed along the y and z axes, respectively. Hydrogen bonds are drawn as dotted lines.

p -electron delocalization within the whole chelation. Also, chelation increases the lipophilic nature of the central atom which subsequently favors its permeation through the lipid layer of the cell membrane [19]. The quantitative assays gave MIC values in the range $3.125\text{--}50\text{ mg mL}^{-1}$, that confirmed the above obtained results.

In summary, the present paper reports the synthesis, characterization and crystal structures of two new iron(III) complexes with Schiff bases. The complexes show effective antibacterial activities against Gram-positive bacteria *S. agalactiae* and *S. aureus* and Gram-negative bacteria *K. pneumoniae* and *P. aeruginosa*. Further work might be carried out to explore

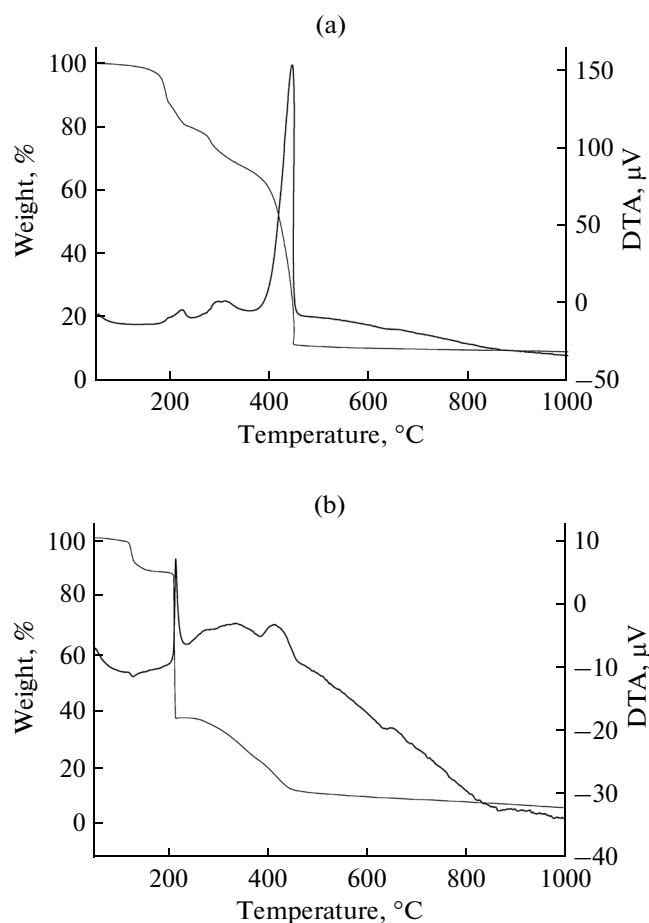


Fig. 3. TG–DTA curves of complexes I (a) and II (b).

more effective antibacterial materials based on the present complex models.

ACKNOWLEDGMENTS

We acknowledge the Education Office of Shanxi Province (project no. 11JK0601) and the Natural Science Foundation of China (project no. 21173003) for supporting this work.

REFERENCES

1. Kuznetsov, I.A., Rasulov, M.M., and Iskakova, J.T., *Bull. Exp. Biol. Med.*, 2013, vol. 154, no. 5, p. 618.
2. Rosenberg, J.T., Sellgren, K.L., Sachi-Kocher, A., et al., *Cytotherapy*, 2013, vol. 15, no. 3, p. 307.
3. Gera, T., Sachdev, H.S., and Boy, E., *Am. J. Clin. Nutr.*, 2012, vol. 96, no. 2, p. 309.
4. Liu, Z.D., Kayyali, R., Hider, R.C., et al., *J. Med. Chem.*, 2002, vol. 45, no. 3, p. 631.
5. Saleem, K., Wani, W.A., and Haque, A., *Future Med. Chem.*, 2013, vol. 5, no. 2, p. 135.
6. Begum, M.S.A., Saha, S., Nethaji, M., et al., *J. Inorg. Biochem.*, 2010, vol. 104, no. 4, p. 477.
7. Dubey, R.K., Dubey, U.K., and Mishra, S.K., *J. Coord. Chem.*, 2011, vol. 64, no. 13, p. 2292.
8. Gu, Z.-G., Na, J.-J., Bao, F.-F., et al., *Polyhedron*, 2013, vol. 51, no. 1, p. 186.
9. Bhattacharjee, C.R., Goswami, P., Sengupta, M., *J. Coord. Chem.*, 2010, vol. 63, no. 22, p. 3969.
10. Saghatforoush, L.A., Aminkhani, A., and Chalabian, F., *Transition Met. Chem.*, 2009, vol. 34, no. 8, p. 899.
11. Sheldrick, G.M., *Acta Crystallogr., A*, 2008, vol. 64, no. 1, p. 112.
12. Indu, M.N., Hatha, A.A.M., Abirosh, C., et al., *Braz. J. Microbiol.*, 2006, vol. 37, no. 2, p. 153.
13. Failes, T.W. and Hambley, T.W., *J. Inorg. Biochem.*, 2007, vol. 101, no. 3, p. 396.
14. Salmon, L., Bousseksou, A., Donnadiou, B., and Tuchagues J.-P., *Inorg. Chem.*, 2005, vol. 44, no. 6, p. 1763.
15. Hayami, S., Miyazaki, S., Yamamoto, M., et al., *Bull. Chem. Soc. Jpn.*, 2006, vol. 79, no. 3, p. 442.
16. Tissot, A., Bertoni, R., Collet, E., et al., *J. Mater. Chem.*, 2011, vol. 21, no. 45, p. 18347.
17. Zhou, Y.-M., Ye, X.-R., Xin, F.-B., et al., *Transition Met. Chem.*, 1999, vol. 24, no. 1, p. 118.
18. Percy, G.C. and Thornton, D.A., *J. Inorg. Nucl. Chem.*, 1972, vol. 34, no. 11, p. 3357.
19. Searl, J.W., Smith, R.C., and Wyard, S., *J. Proc. Phys. Soc.*, 1961, vol. 78, no. 505, p. 1174.